

Measurement of Extreme Hyperfine Fields in Two-Coordinate High-Spin Fe^{2+} Complexes by Mössbauer Spectroscopy: Essentially Free-Ion Magnetism in the Solid State

Aimee M. Bryan,[†] Chun-Yi Lin,[†] Michio Sorai,^{*,‡} Yuji Miyazaki,[‡] Helen M. Hoyt,[§] Annelise Hablutzel,[§] Anne LaPointe,^{||} William M. Reiff,^{*,⊥,#,∇} Philip P. Power,^{*,†} and Charles E. Schulz^{*,§}

[†]Department of Chemistry, University of California at Davis, Davis, California 95616, United States

[‡]Research Center for Structural Thermodynamics, Osaka University, Osaka 560-0043, Japan

[§]Department of Physics, Knox College, Galesburg, Illinois 61401, United States

[⊥]Department of Chemistry, Northeastern University, Boston, Massachusetts 02115, United States

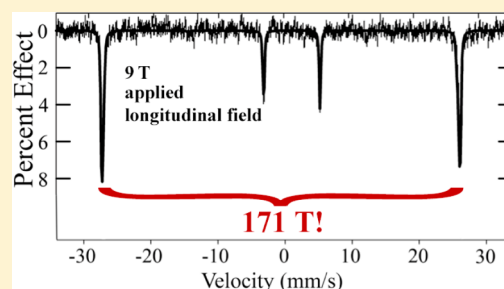
[#]Department of Chemistry and Chemical Biology, Harvard University, Cambridge, Massachusetts 02138, United States

[∇]National High Magnetic Field Laboratory, Tallahassee, Florida 32310, United States

^{||}Department of Chemistry, Cornell University, Ithaca, New York 14853, United States

Supporting Information

ABSTRACT: Mössbauer studies of three two-coordinate linear high-spin Fe^{2+} compounds, namely, $\text{Fe}\{\text{N}(\text{SiMe}_3)(\text{Dipp})\}_2$ (**1**) (Dipp = C_6H_3 -2,6- Pr_2), $\text{Fe}(\text{OAr}')_2$ (**2**) [$\text{Ar}' = \text{C}_6\text{H}_3$ -2,6-(C_6H_3 -2,6- Pr_2) $_2$], and $\text{Fe}\{\text{C}(\text{SiMe}_3)_3\}_2$ (**3**), are presented. The complexes were characterized by zero- and applied-field Mössbauer spectroscopy (**1–3**), as well as zero- and applied-field heat-capacity measurements (**3**). As **1–3** are rigorously linear, the distortion(s) that might normally be expected in view of the Jahn–Teller theorem need not necessarily apply. We find that the resulting very large unquenched orbital angular momentum leads to what we believe to be the largest observed internal magnetic field to date in a high-spin iron(II) compound, specifically +162 T in **1**. The latter field is strongly polarized along the directions of the external field for both longitudinal and transverse field applications. For the longitudinal case, the applied field increases the overall hyperfine splitting consistent with a dominant orbital contribution to the effective internal field. By contrast, **2** has an internal field that is not as strongly polarized along a longitudinally applied field and is smaller in magnitude at ca. 116 T. Complex **3** behaves similarly to complex **1**. They are sufficiently self-dilute (e.g., $\text{Fe}\cdots\text{Fe}$ distances of ca. 9–10 Å) to exhibit varying degrees of slow paramagnetic relaxation in zero field for the neat solid form. In the absence of EPR signals for **1–3**, we show that heat-capacity measurements for one of the complexes (**3**) establish a g_{eff} value near 12, in agreement with the principal component of the ligand electric field gradient being coincident with the z axis.



INTRODUCTION

A growing body of work on two-coordinate, first-row, open-shell transition-metal complexes shows that such complexes can display unusual magnetic behavior. Recent reviews^{1,2} have detailed their synthesis, as well as their structural, spectroscopic, and magnetic properties.^{3–15} The unusual effects of two-coordination on their magnetism arise from the fact that, in a linearly coordinated transition-metal complex, both ligands lie along a single axis (by convention the z axis) and, as a result, they do not interfere with electron circulation involving orbitals (i.e., $d_{x^2-y^2}$, d_{xy} , d_{xz} , and d_{yz}) that do not lie directly along the z axis. For example, for a linearly coordinated Fe^{2+} ion, the orbital moment arising from the circulation of the odd electron in the $d_{x^2-y^2}$, d_{xy} orbital (Figure 1) remains unquenched, and as a result, essentially free-ion magnetism is possible.

Among the most studied complexes have been those of Fe^{2+} (d^6 , $S = 2$) and Co^{2+} (d^7 , $S = 3/2$), which have been shown to

display unusually high orbital moments as well as large negative axial zero-field splittings.^{3–15} The latter can be related to the barriers to spin reversal through the relationship $U_{\text{eff}} = |S^2D|$ and thus offer the possibility of the realization of single-molecule magnetism at moderate temperatures. However, there is little information on the relationship between the zero-field splittings, the orbital magnetism, and the magnitude of the magnetic fields within molecules. Such information is crucial to the development of an understanding of the factors that govern molecular spin reversal. A previous ac magnetic study of a series of two-coordinate Fe^{2+} complexes showed that the iron ligands exert a large effect on both the zero-field splitting and the barrier to spin reversal.¹² As described in the Supporting Information (SI), the application of the $S = 2$ spin Hamiltonian

Received: August 6, 2014

Published: November 4, 2014

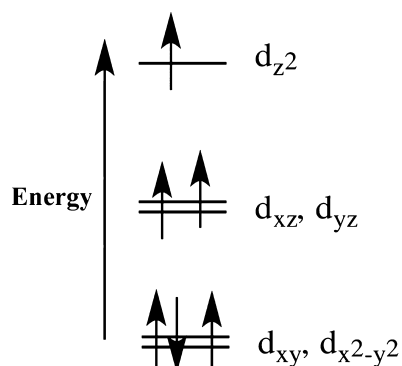


Figure 1. Simplified model of the d^6 electron configuration in the crystal field of a rigorously linear Fe^{2+} complex.

formalism with its corresponding zero-field splitting parameters to the complexes reported here is problematic, because of the orbitally degenerate nature of the ground state. A simple crystal-field model¹⁶ including spin-orbit coupling for the state shown in Figure 1 predicts a spin-orbital ground doublet consisting of the states $|M_L M_S\rangle = |2\ 2\rangle$ and $|-2\ -2\rangle$, which should most appropriately be described by an effective spin $S' = 1/2$. The iron complexes have the advantage that they can generally be studied readily by Mössbauer spectroscopy. This technique can provide highly useful information on the bonding, as well as the electronic and magnetic properties, including the internal magnetic fields in the complexes. Herein, we report Mössbauer measurements to characterize the magnetic properties of the set of two-coordinate $\text{Fe}(\text{II})$ complexes $\text{Fe}\{\text{N}(\text{SiMe}_3)(\text{Dipp})\}_2$ (**1**) ($\text{Dipp} = \text{C}_6\text{H}_3-2,6\text{-}i\text{Pr}_2$),^{1,9,12} $\text{Fe}(\text{OAr}')_2$ (**2**) [$\text{Ar}' = \text{C}_6\text{H}_3-2,6\text{-}(\text{C}_6\text{H}_3-2,6\text{-}i\text{Pr}_2)_2$],¹⁵ and $\text{Fe}\{\text{C}(\text{SiMe}_3)_3\}_2$ (**3**) (Figure 2).^{4,17,18}

In addition, although neither **1**, **2**, nor **3** displays EPR signals, we show that heat-capacity measurements on **3** establish that it has a g_{eff} value near 12, consistent with the principal component of the electric field gradient lying along the z axis.

EXPERIMENTAL SECTION

Mössbauer spectra were measured at 4.2 K using a SeeCo Mössbauer spectrometer, a 100 mCi $^{57}\text{Co}/\text{Rh}$ γ -ray source from Cyclotron Instruments, and a Janis Super Varitemp cryostat with a 0–9 T Nb–Ti superconducting magnet capable of supplying a field parallel to the (vertical) γ -ray beam. Spectra at higher temperatures were recorded using a CryoIndustries closed-cycle cryostat, with a fixed 500 G magnetic field perpendicular to the γ -ray beam. Heat-capacity measurements in an external magnetic field of up to 5 T were carried out for

complex **3** using the Quantum Design physical property measurement system (PPMS 6000) at Osaka University. The compounds $\text{Fe}\{\text{N}(\text{SiMe}_3)(\text{Dipp})\}_2$ (**1**),^{1,9,12} $\text{Fe}(\text{OAr}')_2$ (**2**),^{12,15} and $\text{Fe}\{\text{C}(\text{SiMe}_3)_3\}_2$ (**3**)^{17,18} were prepared according to literature procedures.

RESULTS AND DISCUSSION

Mössbauer Measurements and Spectra. The applied-field spectra for complex **1** are shown in Figure 3. The diminution of the intensity of two of the six allowed transitions (transitions 2 and 5, i.e., the $\Delta m_l = 0$ transitions) of a typical Fe^{57} Zeeman spectrum is diagnostic of the internal magnetic field at the nucleus being aligned parallel to the direction of γ -ray propagation,¹⁹ a process largely completed with an applied field of only 1 T for complex **1** in Figure 3a. There is no evidence of long-range magnetic order in zero field for this sample (see above). The likely explanation for the observed behavior is that there is a readily induced texture effect owing to the fact that complexes **1** and **3** are basically uniaxial in nature (see the g values in Table 1).

The microcrystals in the powder samples apparently easily align with the applied magnetic field. By contrast, for a magnetic field perpendicular to the γ -ray beam (Figure 3b), spectral transitions 2 and 5 are strongly present, that is, enhanced relative to the longitudinal spectrum, as the sample polycrystals, still aligned along the external field, are therefore perpendicular to the γ -ray beam and have an angular intensity coefficient of $2 \sin^2 \theta$, which is ideal in leading to this particular intensity result, namely, the facile observation of all six Mössbauer γ transitions. Furthermore, we note that the overall magnetic hyperfine splitting increases with the increase in the externally applied field. This is as expected when there is a dominant (positive) orbital contribution (H_L), as discussed in the SI.

The spectra for complex **1** were well fit with an effective $S = 1/2$ spin Hamiltonian model (see eq 3, SI) with the fit parameters given in Table 1. In the simulations, powder integration was performed over only angles within 10° of the applied-field axis. Even though the quadrupole splitting in the simulations is negative, the spectra are sensitive only to the component of the electronic field gradient along the z axis, so, in principle, neither the quadrupole splitting nor the asymmetry parameter η are well determined for this system. However, given the high symmetry of the molecule, it is plausible that the asymmetry parameter, η , is close to 0 and that the principal component of the electric field gradient tensor lies along the z axis, for which $g_z = 12$ (see below in the discussion of heat capacity).

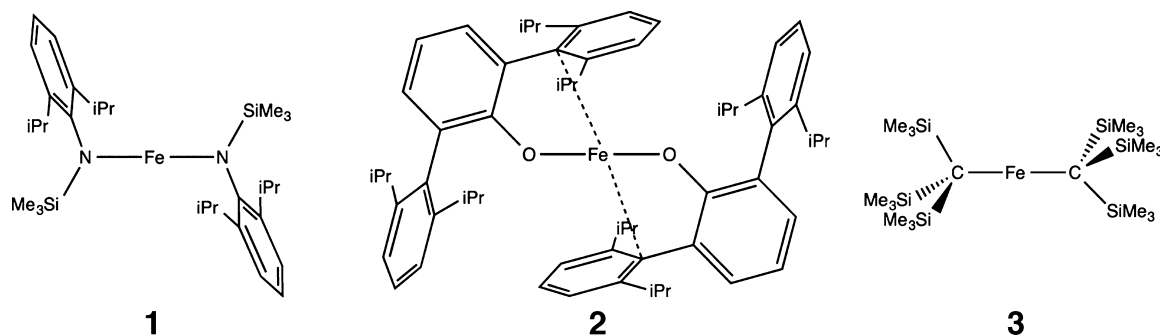


Figure 2. Schematic drawings of compounds **1**–**3**.

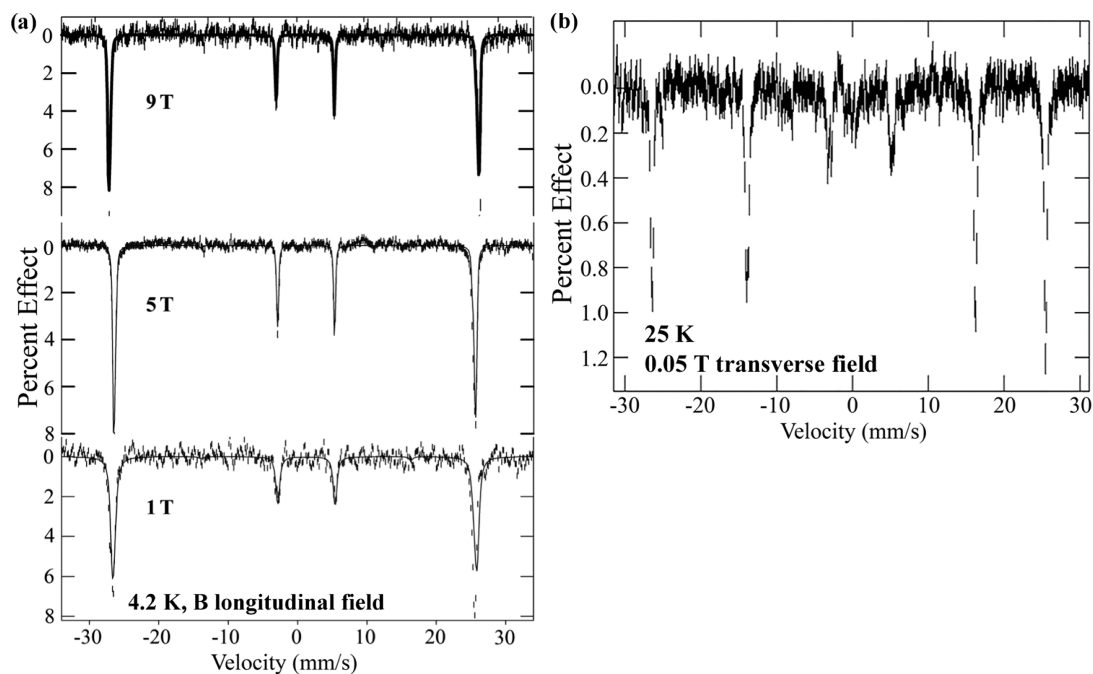


Figure 3. Mössbauer spectra of **1** (a) in 1, 5, and 9 T longitudinal magnetic fields at 4.2 K and (b) in a 0.05 T transverse magnetic field at 25 K.

Table 1. Mössbauer Spectral Parameters for **1–3**

parameter	1	2	3
quadrupole splitting (mm/s)	−1.66	2.25	−1.27
electronic field gradient asymmetry η	0	0.4	0
Isomer shift at 4.2 K (mm/s)	0.41	0.78	0.46
g_{eff}	(0, 0, 12)	(8, 1, 10)	(0, 0, 12)
$A_{xx}/(g_n\beta_n)$ (T)	<i>a</i>	204	<i>a</i>
$A_{yy}/(g_n\beta_n)$ (T)	<i>a</i>	−205	<i>a</i>
$A_{zz}/(g_n\beta_n)$ (T)	324	232	292
internal field H_{int} (T)	162	116	146
Euler angles $g \rightarrow A$ (α, β, γ) (deg)	NA	(−63, 84, 18)	NA

^aUnknown due to large magnetic polarization anisotropy.

Finally, we note that the magnitude of the internal hyperfine field, $A_{zz}S_z/(g_n\beta_n)$, is 162 T (the measured effective field of 171 T in Figure 4 includes the 9 T applied field); to our knowledge, this is the largest value of internal hyperfine field observed to date for a paramagnetic iron-containing compound regardless of spin or oxidation level. It seems clear that this extraordinary result must be more than a fortuitous combination of orbital and spin effects. The field is greater than those observed in the essentially linearly coordinated amides $\text{Fe}(\text{N}^t\text{Bu}_2)_2$ (113 T)⁵ and $\text{Fe}\{\text{N}(\text{H})\text{C}_6\text{H}_3\text{-}2,6(\text{C}_6\text{H}_2\text{-}2,4,6\text{-}i\text{Pr}_3)_2\}_2$ (130 T)⁶ or in the bent geometry $\text{Fe}\{\text{N}(\text{H})\text{C}_6\text{H}_2\text{-}2,4,6\text{-}\text{Me}_3\}_2$ (73 T).⁶ The greater field observed in **1** might be associated with the shorter Fe–N bonds [1.851(4) Å] in this compound, in comparison to 1.880(2) Å in $\text{Fe}(\text{N}^t\text{Bu}_2)_2$ ⁵ and 1.901(14) Å in $\text{Fe}\{\text{N}(\text{H})\text{C}_6\text{H}_3\text{-}2,6(\text{C}_6\text{H}_2\text{-}2,4,6\text{-}i\text{Pr}_3)_2\}_2$.⁶ It has been proposed that the shorter Fe–N distance in **1** might be due to attractive dispersion forces between the ligand substituents.⁹ A comparison (Figure 4) of the internal magnetic field in **1** with that of iron in iron foil underlines the large effect produced by the linear two-coordination environment of the Fe^{2+} ion in **1**.

In contrast to the Mössbauer spectra of **1**, those of **2** (Figure S) tell a different story. A significantly larger applied field is needed for the spectra to exhibit resolved magnetic hyperfine

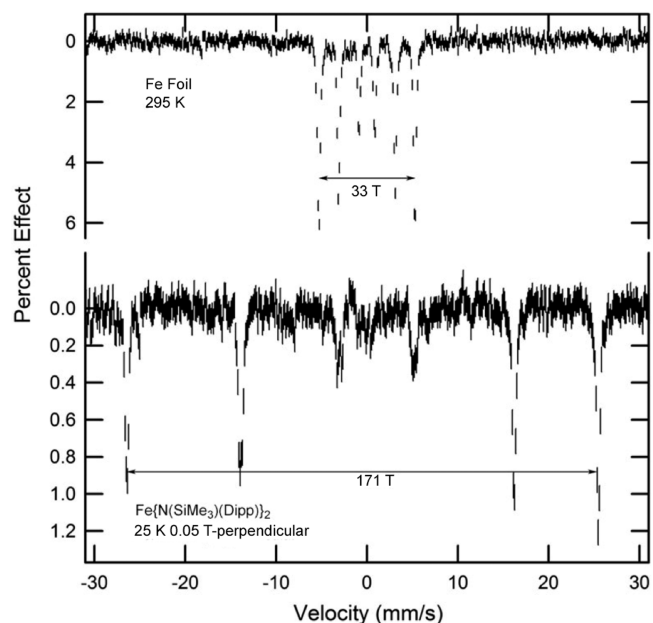


Figure 4. Comparison of internal field of **1** with that of α -iron foil, the standard velocity calibrant for ^{57}Fe Mössbauer studies.

splitting at 4.2 K (i.e., for the system to be in the slow relaxation limit), and the persistent intensity of transitions 2 and 5 ($\Delta m_1 = 0$) as measured in a field parallel to the γ rays argues against the induction of the texture effect seen in **1**. Fit parameters for **2** are also reported in Table 1.

We note from Figure 2 that, unlike complexes **1** and **3**, complex **2** [$\text{Fe}-\text{O} = 1.8472(9) \text{ \AA}^{15}$] also has two possible ipso-carbon interactions with the flanking aryl rings off the z axis that have a relatively close [2.765(3) Å] equatorial approach to the iron atom and can thus be expected to lower the symmetry of the ligand field at the complex, the linear character of the O–Fe–O bond notwithstanding. The relatively large isomer shift of **2** ($\delta = 0.78 \text{ mm}^{-1}$) argues for the existence of the secondary

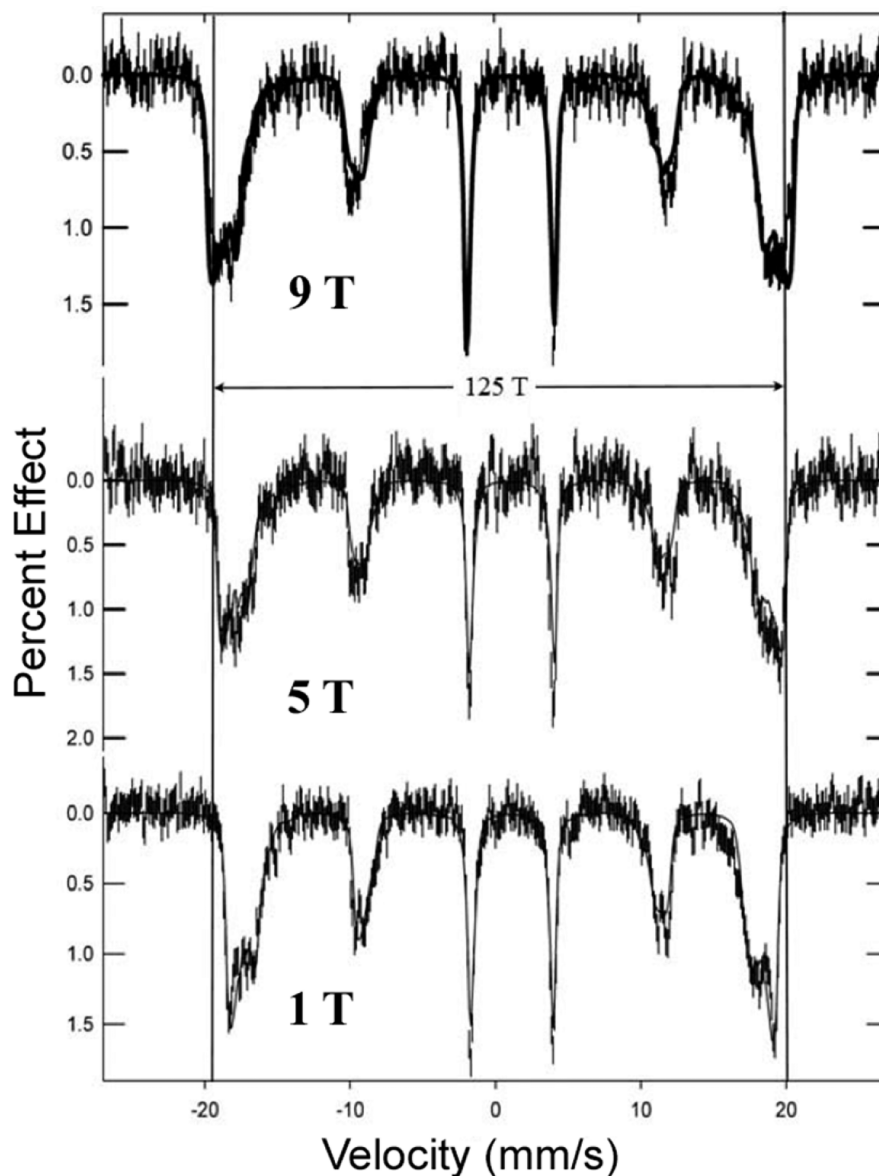


Figure 5. Mössbauer spectra of **2** in 1, 5, and 9 T longitudinal magnetic fields at 4.2 K.

Fe–C(ipso) interactions (although calculations indicate that they are weak), and the structure is consistent with that expectation. The δ value resembles the 0.76 mm^{-1} value found in $\text{Fe}\{\text{N}(\text{H})\text{Ar}^{\text{Me}_6}\}_2$, which has close Fe \cdots C interactions near 2.69 \AA . The fits to the Mössbauer spectra of this complex did not require inclusion of a texture effect but did require Euler angle rotations of the effective $S' = 1/2$ g tensor with respect to the A tensor.

The fact that the quadrupole splitting, determined by the fit to the spectrum, has the opposite sign for complex **2** is evidence that the secondary interactions of the C(ipso) atoms have a significant effect on the Fe site. The effective doubling of the outer lines (i.e., lines 1 and 6; $\Delta m_l = \pm 1$ transitions) of the Mössbauer spectrum is an indication of low symmetry at the iron site. Although susceptibility data and Mössbauer data imply that complex **2** has no long-range magnetic order, such doubling of the outer lines has also been seen in magnetically ordered network systems that have anisotropy (e.g., similar to ferromagnetic cubic pyrochlore FeF_3 networks whose magnetic structure is largely impervious to strong external fields).²⁰

Similar substantial resistance to the polarization effects of large external magnetic fields are observed for the Mössbauer spectrum of the ferromagnetically ordered decamethyl ferrocenium tetracyanoethylene chain, whose low-spin Fe^{3+} cation $[\text{Fe}(\text{Cp}^*)_2]^+$ ($\text{Cp}^* = \eta^5\text{-C}_5\text{Me}_5$) exhibits strong g -factor anisotropy and, likewise, doubling of the ($\Delta m_l = \pm 1$) γ -ray transitions.²¹

An interesting feature of these species is that, although they are non-Kramers systems, the degeneracy of the ground-state doublet causes them to behave similarly to Kramers systems in that one expects a complete polarization of the spin and orbital moments even in quite small applied fields. A consequence of this is that the magnitude of the internal field at the nucleus is independent of applied field; thus, as the external applied field is increased, the effective field ($H_{\text{int}} + H_{\text{applied}}$) increases, as expected, by the same amount.

The applied-field spectra of complex **3** are shown in Figure 6 (a zero-field Mössbauer spectrum of **3** was previously published by us in ref 4; see also ref 14). These spectra resemble those of **1**. The increasing velocity separations of transitions 1 and 6 as a

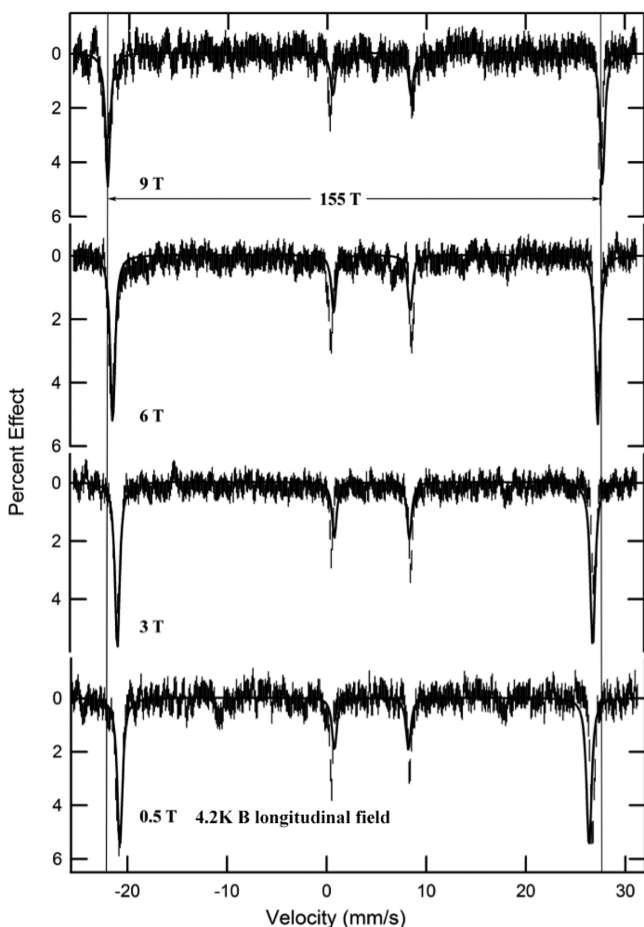


Figure 6. Mössbauer spectra of **3** in 0.5, 3, 6, and 9 T longitudinal magnetic fields at 4.2 K. (The measured 155 T in the top spectrum includes the 9 T applied field, so that the actual internal field is 146 T.)

function of increasing longitudinal applied field for both complexes **1** and **3** clearly confirm a dominant positive orbital contribution to their internal hyperfine fields. Needless to say, the relation of the magnitude of the internal hyperfine fields to the specific identity of the Fe²⁺-bonded ligand atoms is not obvious for this series of complexes based on the present data. Although there are no significant distortions from linear symmetry in the complexes, the variations in internal field strength might be related to the overall symmetry of the complexes (e.g., *D*_{3d} vs *C*_{2h} symmetry) or differences in anisotropic covalency among the 3d orbitals.³ In any event, it is informative to enumerate the contributions to the internal hyperfine field for complexes **1**–**3** at this juncture. Given the ratios of the three contributions to the internal field (see eq 7, SI), one can calculate the magnitudes of the internal field components, which are given in Table 2. We note that R[−] and NR₂[−] are strong-field ligands compared to OR[−], which is comparable to the weak-field halogen-ion ligands. In effect, the crystal-field splitting is in the order R[−] > NR₂[−] > OR[−]. The

Table 2. Internal Field Components for **1**–**3**

compound	<i>H</i> _{int} (T)	<i>H</i> _L (T)	<i>H</i> _{dipolar} (T)	<i>H</i> _{contact} (T)
Fe{N(SiMe ₃)(Dipp)} ₂ (1)	162	204	29	−71
Fe(OAr') ₂ (2)	116	146	21	−51
Fe{C(SiMe ₃) ₃ } ₂ (3)	152	192	27	−67

data given in Table 2 have the ordering NR₂[−] > R[−] > OR[−] for the internal fields. However, the position of NR₂[−] [i.e., N(SiMe₃)Dipp[−]] in this series is probably anomalous, because of the shortening of the Fe–N bonds by dispersion forces as described above.⁹ Instead, the internal fields observed in Fe{N(H)C₆H₃-2,6(C₆H₂-2,4,6-^{*i*}Pr₃)₂}₂ (130 T)⁶ and Fe-(N^{*t*}Bu₂)₂ (113 T),⁵ as discussed above, are probably more representative of the fields normally produced by amido ligands. Given the lower symmetry of complex **2**, the assumptions about the nonadmixed ground state (see eq 6, SI) do not necessarily apply to this system. Nonetheless, the overall internal field, determined by the magnetic hyperfine splitting, should be accurate as given in Table 2.

In addition to the striking difference in the magnitudes of the internal fields of complexes **1** and **2**, there is a corresponding difference in spin relaxation rates owing to intrinsic differences in the natures of the ground states. For instance, if the ground doublet states were pure |*M*_L*M*_S) = |±2 ±2) states (i.e., if they did not have significant admixtures of excited states due to low-symmetry ligand-field components or covalency effects), then spin–lattice transitions would be strongly forbidden, as is required for |Δ*M*_J| = 8 transitions. (cf. the ground state pictured at the bottom of Figure S1, SI). In contrast, when the ground doublet wave functions do become admixed with excited states, for example, through a rhombic field potential, direct spin–lattice transitions as well as Orbach and Raman processes become more probable. Such admixed wave functions are also expected to result in smaller orbital contributions to the internal field at iron. The differences between the 4.2 K, zero-field Mössbauer spectra of complexes **1** and **2** (Figure 7) are consistent with these expectations.

Heat-Capacity Measurements for 3. Heat-capacity measurements afford an opportunity to verify that the ground state of a system is a degenerate doublet that can be characterized with an effective *g* value. For a material with a ground-state doublet having an energy separation Δ between the states of the doublet, there will be a contribution to the molar heat capacity of the material described as a Schottky anomaly:²²

$$C_p = R \left(\frac{\Delta}{kT} \right)^2 \frac{e^{\Delta/kT}}{(1 + e^{\Delta/kT})^2}$$

where *R* is the gas constant, 8.315 J/(mol·K). If the ground state is degenerate in the absence of an applied magnetic field, then in the presence of a field *H*, the energy splitting can be described in terms of an effective *g* value: Δ = *g*_{eff}μ_B*H*. Thus, study of the Schottky anomaly can verify both the degeneracy of the ground doublet in these linear molecules and also the prediction that *g*_{eff} = 12.

Figure 8a (from 300 to ~0.1 K) and Figure 8b (from 50 to ~0.5 K) correspond to zero-field constant-pressure molar heat-capacity measurements for compound **3** in an independent determination of whether the hyperfine splitting of its low-temperature Mössbauer spectra (see above) owes to genuine cooperative long-range magnetic order at low *T* or perhaps is due to slow single-ion paramagnetic relaxation. Because we do not have an isomorphous diamagnetic analogue for **3** (or for **1** or **2** for that matter), we cannot correct for a lattice heat-capacity contribution to *C*_p versus *T* as part of a search for a sharp lambda anomaly that often accompanies long-range magnetic order. On the other hand, superconducting quantum interference device (SQUID) magnetization studies of **1**–**3**

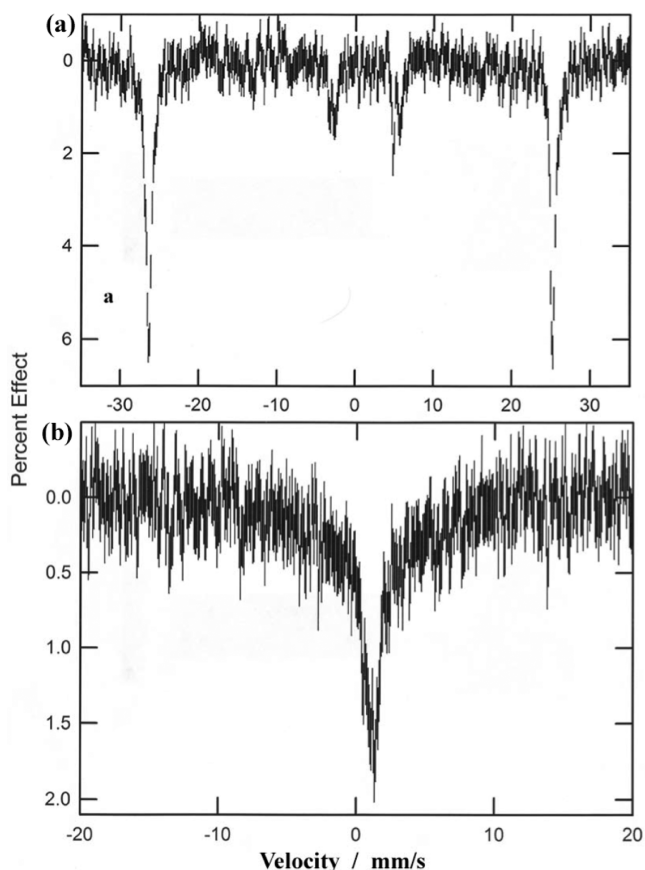


Figure 7. Mössbauer spectra of (a) complex 1 and (b) complex 2 at 4.2 K in zero applied field.

conducted by us and others^{4,12} give no clear evidence of long-range magnetic order. In this context, there are no obvious direct structural or superexchange pathways that lead one to predict long-range order for these systems within temperatures accessible given our current laboratory capabilities. In the

absence of an apparent lambda anomaly for these compounds, we conclude that they have no long-range magnetic order.

In Figure 9, we show the resulting graphs of $C_p(H) - C_p(0)$ as a function of temperature for applied fields of $H = 0.5, 1.0,$

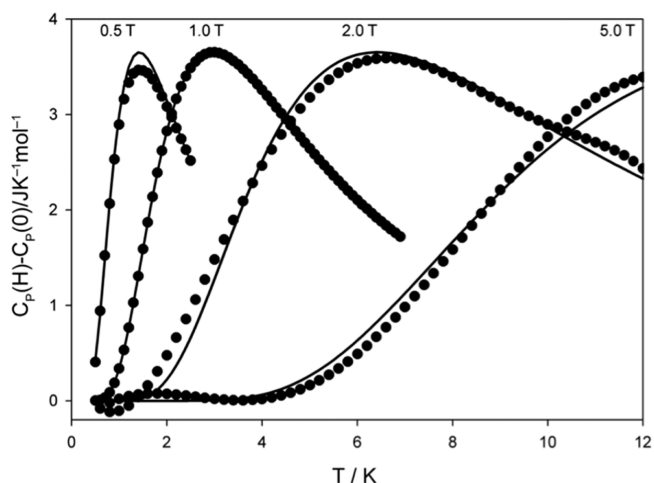


Figure 9. Plot of $C_p(H) - C_p(0)$ at fields of 0.5, 1.0, 2.0, and 5.0 T versus temperature.

2.0, and 5.0 T. Each of the data sets was fit as a Schottky anomaly, with a least-squares procedure being used to determine the four values for the parameter Δ . In Figure 10, a linear regression of Δ versus H yielded a value of $g_{\text{eff}} = 11.2 \pm 0.2$, with a linear correlation coefficient of $R = 0.9997$. The intercept of the regression is -0.20 ± 0.33 , consistent with zero—that is, consistent with a degenerate ground doublet. This result provides evidence that the ground state is in fact a doublet, namely, $M_J = \pm 4$, which is electron-spin-resonance- (ESR-) silent in view of $\Delta M_J = 8$ (Figure S1, SI).²³ The resulting g_{eff} value is very close to the expected value of 12.0, strongly supporting the proposed model for this system and, finally, completely consistent with a very large ground-

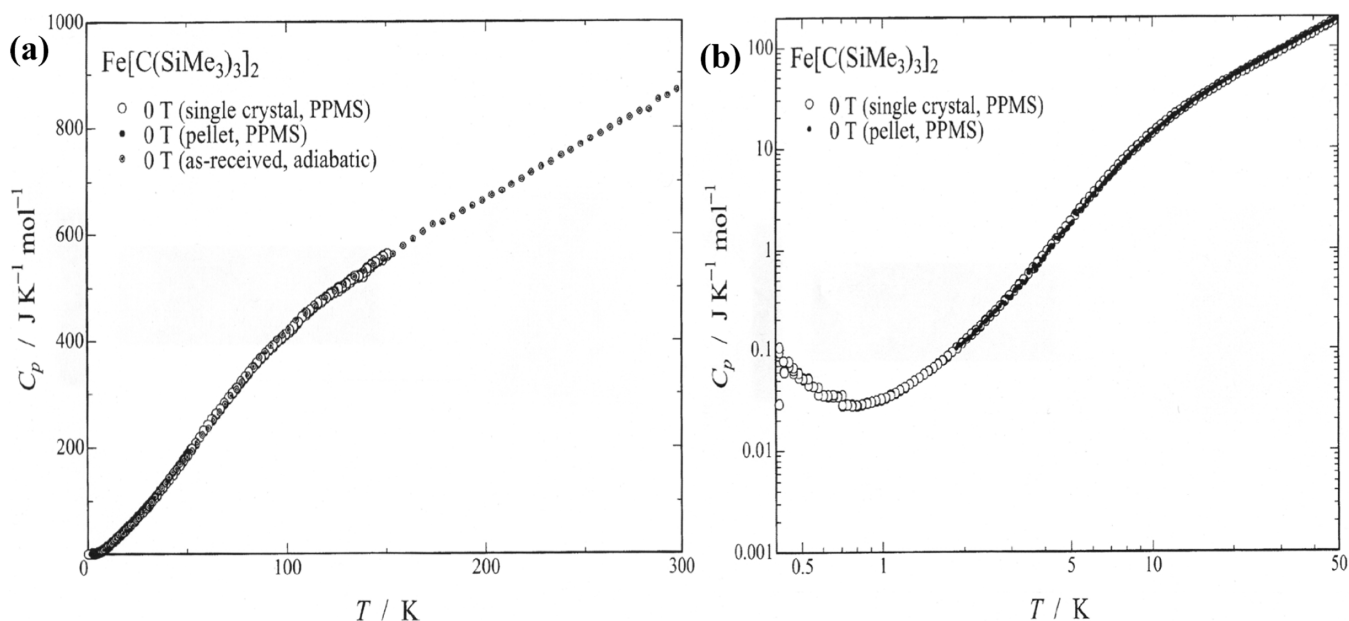


Figure 8. Plots of the heat capacity of 3 versus temperature on (a) linear and (b) logarithmic scales.

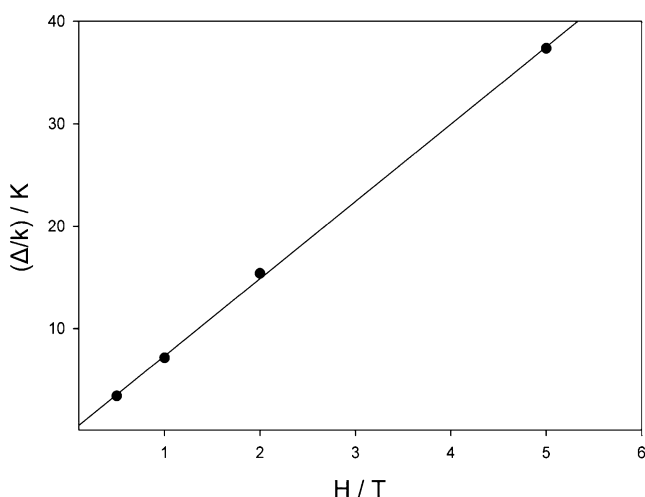


Figure 10. Linear regression of Δ versus H .

state first-order orbital angular momentum. That is, apparently, the two axial ligands present in compounds **1** and **3** are sufficiently isolated (Fe^{2+} –ligand distances of ca. 2 Å) as to do little to quench the strong first-order orbital angular momentum of the extra electron in the xy plane. In a very real sense, this, in turn, allows for the magnetic moment of these systems to approach that of the corresponding free gas-phase ferrous ion. In this context, recall that the spin-only moment for high-spin Fe^{2+} is ca. $4.9 \mu_{\text{B}}$ whereas the free-gas-phase-ion value is ca. $6.70 \mu_{\text{B}}$.²⁴ The moments measured by SQUID magnetometry for complexes **1** and **3** are ca. $6.20 \mu_{\text{B}}$ and $6.48 \mu_{\text{B}}$, respectively, that is, some 93% and 97%, respectively, of the free-ion values (6.7 and $6.63 \mu_{\text{B}}$, respectively). These large values of μ_{eff} correlate well with the respective extraordinarily large internal hyperfine fields for the Mössbauer spectra at 4.2 K (see above, Table 1), as do their relaxation barriers.^{12a} Herein, we also note that the effective moment for **2** is somewhat smaller at $5.29 \mu_{\text{B}}$ (78% of the free-ion value) with $H_{\text{int}} \approx 116$ T.

CONCLUSIONS

In conclusion, we emphasize the very large magnitude of the internal fields in complexes **1–3**. In contrast to the internal field of some 33 T felt by the iron nuclei in (ferromagnetically ordered) α -iron foil, the iron nucleus experiences a field of 162 T, nearly 5 times as large, in complex **1** (Figures 3 and 4). It is clearly of interest to better understand how the role of the nature of the various ligand atoms affects the magnitude of the internal fields in these compounds. Density functional theory calculations might be a reasonable modality for achieving such an understanding.²³

ASSOCIATED CONTENT

Supporting Information

Background information for the magnetism of linearly coordinated Fe^{2+} complexes. This material is available free of charge via the Internet at <http://pubs.acs.org>.

AUTHOR INFORMATION

Corresponding Authors

*E-mail: sorai@chem.sci.osaka-u.ac.jp (M.S.).

*E-mail: w.reiff@neu.edu (W.M.R.).

*E-mail: pppower@ucdavis.edu (P.P.P.).

*E-mail: cschulz@knox.edu (C.E.S.).

Notes

The authors declare no competing financial interest.

ACKNOWLEDGMENTS

We thank the National Science Foundation (Grant CHE-1263760) for support of this work.

REFERENCES

- (1) (a) Power, P. P. *Chem. Rev.* **2012**, *112*, 3482. (b) Power, P. P. *Comments Inorg. Chem.* **1989**, *8*, 177.
- (2) Kays, D. L. *Dalton Trans.* **2011**, *40*, 769.
- (3) Layfield, R. A. *Organometallics* **2014**, *33*, 1084.
- (4) Reiff, W. M.; La Pointe, A. M.; Witten, E. H. *J. Am. Chem. Soc.* **2004**, *126*, 10206.
- (5) Reiff, W. M.; Schulz, C. E.; Whangbo, M. H.; Seo, J. L.; Lee, Y.; Potratz, G. R.; Spicer, C. W.; Girolami, G. S. *J. Am. Chem. Soc.* **2009**, *131*, 404.
- (6) Merrill, W. A.; Stich, T. A.; Brynda, M.; Yeagle, G. J.; de Hont, R.; Fettinger, J. C.; Reiff, W. M.; Power, P. P. *J. Am. Chem. Soc.* **2009**, *131*, 12693.
- (7) Ni, C.; Stich, T. A.; Long, G. J.; Power, P. P. *Chem. Commun.* **2010**, *46*, 4466.
- (8) (a) Bartlett, R. A.; Power, P. P. *J. Am. Chem. Soc.* **1987**, *109*, 7563. (b) Bryan, A. M.; Merrill, W. A.; Reiff, W. M.; Fettinger, J. C.; Power, P. P. *Inorg. Chem.* **2012**, *51*, 3366. (c) Boynton, J. N.; Merrill, W. A.; Reiff, W. M.; Fettinger, J. C.; Power, P. P. *Inorg. Chem.* **2012**, *51*, 3212.
- (9) Lin, C.-Y.; Guo, J.-D.; Fettinger, J. C.; Nagase, S.; Grandjean, F.; Long, G. J.; Chilton, N. F.; Power, P. P. *Inorg. Chem.* **2013**, *52*, 13584.
- (10) Bryan, A. M.; Long, G. J.; Grandjean, F.; Power, P. P. *Inorg. Chem.* **2014**, *53*, 2325.
- (11) Lin, C.-Y.; Fettinger, J. C.; Grandjean, F.; Long, G. J.; Power, P. P. *Inorg. Chem.* **2014**, *53*, 9400.
- (12) (a) Zadrozny, J. M.; Atanasov, M.; Bryan, A. M.; Lin, C.-Y.; Rekken, B. D.; Power, P. P.; Neese, F.; Long, J. R. *Chem. Sci.* **2013**, *4*, 125. (b) Atanasov, M.; Zadrozny, J. M.; Long, J. R.; Neese, F. *Chem. Sci.* **2013**, *4*, 139.
- (13) Zadrozny, J. M.; Xiao, D. J.; Atanasov, M.; Long, G. J.; Grandjean, F.; Neese, F.; Long, J. R. *Nat. Chem.* **2013**, *5*, 577.
- (14) Zadrozny, J. M.; Xiao, D. J.; Long, J. R.; Atanasov, M.; Neese, F.; Grandjean, F.; Long, G. J. *Inorg. Chem.* **2013**, *52*, 13123.
- (15) Ni, C.; Fettinger, J. C.; Long, G. J.; Brynda, M.; Power, P. P. *Chem. Commun.* **2008**, *45*, 6045.
- (16) The simple model provides the ordering of the d orbitals according to straightforward crystal-field considerations. However, calculations¹² for a range of two-coordinate Fe^{2+} complexes have shown that the ordering of the quintet energy states most closely associated with the d_z^2 (3A) and d_{xz} , d_{yz} (5E) orbitals can be reversed. However, this does not change the degeneracy of the ground state associated with the unequal occupancy of the d_{xy} and $d_{x^2-y^2}$ orbitals. On the other hand, it has been shown that reduction of linear Fe^{2+} complexes to Fe^+ can lead to the d_z^2 orbital being the most stable, apparently as a result of s–d orbital mixing.¹³ This does not occur in the linear Fe^{2+} complexes, because the ordering $(d_{xz}, d_{yz})^2 > (d_{x^2-y^2}, d_{xy})^2 > (d_z^2)^2$ would be expected to have no ground-state orbital moment. We note also that, although complexes **1–3** all have linear iron coordination, calculations^{12b} have shown that the complexes are on the borderline of a transition from static to dynamic Renner–Teller effects, which can cause a large reduction in the spin-reversal barrier.
- (17) Viehhaus, T.; Schwartz, W.; Hübler, K.; Locke, K.; Weidlein, J. Z. *Anorg. Allg. Chem.* **2001**, *627*, 715.
- (18) La Pointe, A. M. *Inorg. Chim. Acta* **2003**, *345*, 359.
- (19) Greenwood, N. N.; Gibb, T. C. *Mössbauer Spectroscopy*; Chapman & Hall: London, 1971; p 66.
- (20) Calage, Y.; Zemirli, M.; Greneche, J. M.; Varret, F.; De Pape, R.; Ferey, G. *J. Solid State Chem.* **1987**, *69*, 197.

- (21) Reiff, W. M. In *Mössbauer Spectroscopy Applied to Magnetism and Materials Science*; Long, G. J., Grandjean, F., Eds.; Plenum Press: New York, 1993; Vol. 1, p 221.
- (22) Kittel, C. *Introduction to Solid State Physics*; John Wiley & Sons: New York, 1971; p 523.
- (23) Dai, D.; Xiang, H.; Whangbo, M.-H. *J. Comput. Chem.* **2008**, *29*, 2187.
- (24) Drago, R. S. *Physical Methods in Chemistry*; W. B. Saunders: Philadelphia, PA, 1977; p 425.